Rotor Bar Fault Diagnosis by Using Power Factor

Hayri Arabacı, Osman Bilgin and Abdullah Ürkmez

***Abstract*— The paper presents detection and classification of rotor bar faults at steady state operation in squirrel cage induction motor by using power factor. One phase current and voltage of the stator coils were used to calculate the power factor. To investigate effects of rotor faults on the power factor, its frequency spectrum was obtained by fast Fourier Transform (FFT). Significant picks in the spectrum were used to discern "healthy" and "faulty" motor conditions. The motor conditions were classified by Artificial Neural Network (ANN). In experiments three different rotor faults and healthy motor conditions were investigated by 30 HP, 8'', with 18 bars, 380V, 2 poles and 50 Hz squirrel cage submersible induction motor. The proposed decision structure detects and classifies rotor bar faults with 100% accuracy.**

***Index Terms*—Broken rotor bar, fault diagnosis, induction motors, Fast Fourier Transform, Artificial Neural Network.**

I. Introduction

Induction motors are critical component of many industrial processes and are widely used as main drive for most rotating mechanical loads. Most electric motor faults interrupt a process, and may damage other related machinery. During recent years, there has been a substantial amount of research to provide condition monitoring techniques for ac induction motors based on motor current signature analysis (MCSA) [3-5] as current signals can easily be monitored for condition monitoring [5]. The problem is how to extract different features from the current signal and discriminate among various motor conditions. Most of the works on MCSA use second order based techniques like FFT analysis. Some work particularly uses the sidebands around the supply line frequency at twice the slip frequency and its multiples $(1 \pm 2s)f$ in frequency spectrum of the current [6, 7]. The amplitude of the fundamental frequency is considerably greater than the sideband amplitude and the sideband is very close the fundamental frequency component depending on the slip. Therefore, relied solely on current FFT particular solution has only limited ability to make an accurate detection [8]. Recent years, many upgrades of the basic MCSA algorithms have been proposed in order to improve detection accuracy and sensitivity. To solve the problem, two or three phase currents or voltage signals or their combinations have been used [9-12]. To develop such fault-detection, several authors have used modern computing approaches such as neural networks [6], artificial immune system [7].

Therefore, in this paper one phase current and voltage of the stator coils were used to calculate the power factor. To investigate effects of rotor faults on the power factor, its frequency spectrum was obtained by FFT. Significant picks in the spectrum were used to discern "healthy" and "faulty" motor conditions. The motor conditions were classified by ANN.

Manuscript received February 25, 2011. Scientific Research Project Found of Selcuk University has been provided the financial support to this project.

H. Arabacı is with the Department of Electrical and Electronics Engineering, Selcuk University, 42075, Konya, Turkey, (corresponding author's phone: +90-332-2232031; fax: +90-332-2410635; e-mail: hayriarabaci@selcuk.edu.tr).

O. Bilgin is with the Department of Electrical and Electronics Engineering, Selcuk University, 42075, Konya, Turkey (e-mail: obilgin@selcuk.edu.tr).

A. Ürkmez is with the Department of Electrical and Electronics Engineering, Selcuk University, 42075, Konya, Turkey (e-mail: aburkmez@selcuk.edu.tr).

II. Material and Method

The distortion of the rotor's magnetic field orientation and the resulting local saturation in the rotor laminations around the region of the broken bars lead to a quasi-elliptical trace of the magnetic field's space vector. So, stator current is affected according to motor slip as in Equation (1).

$$f_b = (1 \pm 2ks) f \quad , \quad k = 1,2,3,.... \tag{1}$$

Where f is main frequency and s is slip. The effects cause fluctuations on the current. Zero-crossing points of current are changing because of the fluctuations. Therefore, power factor of motor oscillates depend on the slip frequency. The frequency, it occurred by rotor bar faults, is available in multiple of $2sf$ in frequency spectrum of the power factor. The frequency spectrum region was used to detection and classification of rotor bar faults in the present study.

One phase current and voltage of the stator coils were measured to calculate the power factor. The zero-crossing points of the current and voltage and their periods are determined and power factor is calculated by these zero-crossing points and periods according to Equation 1.

$$Power\ factor = \frac{T_d}{T} \tag{1}$$

Where T_d is distance between the current zero-crossing point and the voltage zero-crossing point, T is period of voltage. These values are shown more clearly in Fig. 1.

ISBN: 978-988-19251-4-5
ISSN: 2078-0958 (Print); ISSN: 2078-0966 (Online)

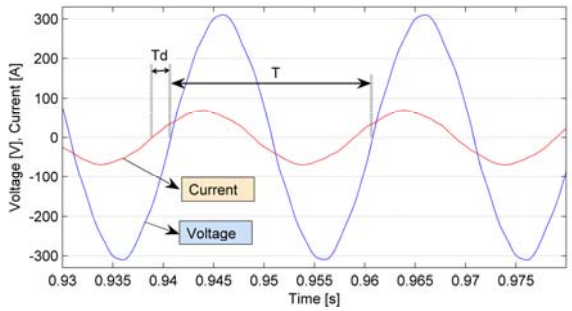

Fig. 1. The zero-crossing points of stator current and voltage and showing of T and T_d.

The power factors are analyzed for each fault size and they are compared with other fault sizes and healthy rotor in time domain as shown Fig. 2.

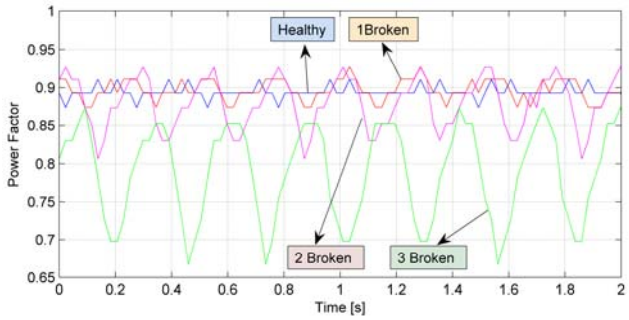

Fig. 2. The power factor variations according to faults size in time domain.

The power factor oscillations in time domain may occur due to changes in motor load. Discerning is needed that these oscillations result from the fault or load change. So, DC components are extracted and then the power factor data in time domain are transformed to frequency domain by FFT. The frequency component corresponding to $2sf$ in the spectrum is useful to feature extraction for detection of rotor bar faults. Fig. 3 shows the frequency spectrum of power factor for faulty and healthy conditions.

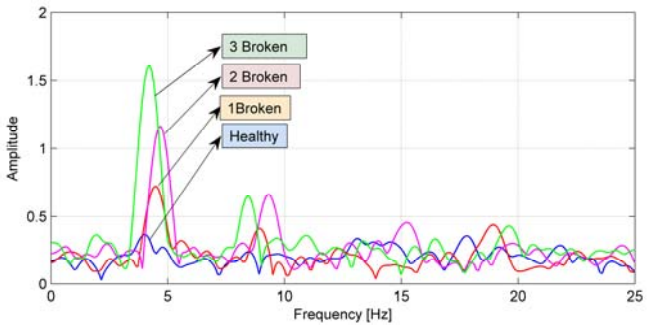

Fig. 3. The frequency spectrum of power factor for faulty and healthy conditions.

Finally, the frequency spectrum of power factor is used to be inputs of ANN. So, the faulty motor conditions are detected and classified by using ANN outputs.

III. Experimental Study and Results

The experiments are made by 30 HP, 8'', with 18 bars, 380V, 2 poles and 50 Hz squirrel cage submersible induction motor. The purposed three different rotor faults were created in the factory at the production phase. The analyzed rotor faults are shown as follows:

- A rotor with one broken rotor bar,
- A rotor with two adjacent broken rotor bars,
- A rotor with three adjacent broken rotor bars.

In order to ensure accurate measurements, each rotor fault was created separately and passed through each assembly phase. To obtain broken rotor bar faults, a small part (5 mm length) is cut from the mid side of rotor bar and the two parts of bar are stacked from both sides. So conductivity of the bar is decreased to 0, as shown in Fig. 4. Broken rotor bar photograph is given in Fig. 5.

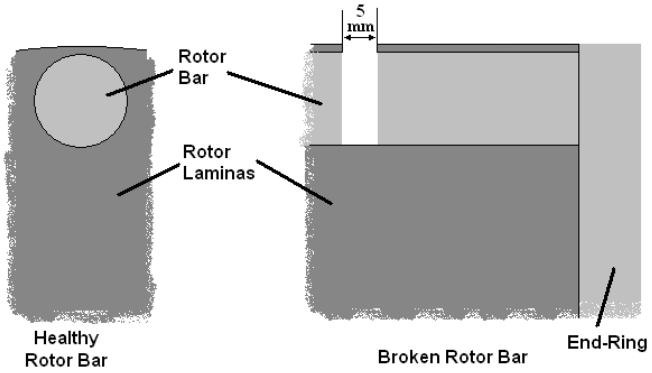

Fig. 4. Obtaining of broken rotor bar.

Fig. 5. Photograph of broken rotor bar parts and rotor.

The motors were tested in the motor factory by using experiment system. The tested motor was loaded by generator. Load is leveled by using resistors which conducted to the generator. The photographs of the used experiment system are given in Fig. 6. One phase current and voltage of the stator coils were obtained to calculate the power factor in steady state operation for each fault.

ISBN: 978-988-19251-4-5
ISSN: 2078-0958 (Print); ISSN: 2078-0966 (Online)

Fig. 6. Photograph of experiment system.

The current and voltage were sampled by using Hall-effect sensors from the tested motor coils. Sampling was made at 7.5 kHz. The data were transformed to frequency domain by using FFT.

A. ANN Training, Test and Results

A feed-forward network trained by back-propagation algorithm was used for classification. Inputs propagate from input layer to output layer via one hidden layer. The frequency spectrums are used as input vector for training the ANN which defines the target as healthy or faulty. After the training, the NN used to detect the faulty motor conditions.

Input matrixes of ANN are the frequency spectrum of power factor (as shown Fig. 3) between 0 and 25 Hz.

Output matrixes of ANN are column matrixes and they consist of 4 components. Every line represents 4 different motor conditions.

Each fault representing output matrixes:

Healthy : $[1\ 0\ 0\ 0\ ]^T$
A broken bar : $[0\ 1\ 0\ 0\ ]^T$
Two broken bars : $[0\ 0\ 1\ 0\ ]^T$
Three broken bars : $[0\ 0\ 0\ 1\ ]^T$

The choosing of output matrix having four components increased accuracy of the diagnosis.

There were eighteen data for every condition. the eight of the data were used for training and other eight data were used for test.

Training and test were implemented at different number of hidden layers and iterations to find optimal number of hidden layers and iterations. Following criteria were used for optimization:

Training Error : Per unit of ratio of difference between real results and training results to number of total samples.

Test Error : Per unit of ratio of difference between real results and test results to number of total samples.

Diagnosis Error : Per unit of ratio of number of mistaken diagnosises to number of total diagnosis.

Healthy Error : Per unit of ratio of number of mistaken diagnosises in healthy motor conditions to number of total diagnosises.

Because of that goal is to detection fault, "Diagnosis Error" was used to be the most significant indicator in the optimization.

TABLE I. THE ERRORS FOR 500 ITERATIONS AT DIFFERENT NUMBER OF HIDDEN LAYER.

Hidden Layer	Healthy Error [%]	Training Error [%]	Test Error [%]	Diagnosis Error [%]
50	0	3.77E-05	1.74E+00	2.78
100	0	1.28E-07	4.30E-01	0
120	0	3.08E-04	2.11E+00	8.33
150	0	1.15E-05	6.00E-01	0
200	0	1.01E-10	1.36E+00	2.78
250	0	2.49E-10	8.50E-01	0
450	0	1.42E-08	2.00E+00	2.78
500	0	3.90E-12	3.30E-01	0
550	0	1.45E-08	1.16E+00	0
750	0	5.86E-12	2.79E+00	2.78

TABLE II. THE ERRORS FOR 100 HIDDEN LAYERS AT DIFFERENT NUMBER OF ITERATIONS.

Iteration Number	Healthy Error [%]	Training Error [%]	Test Error [%]	Diagnosis Error [%]
250	0	6.00E-05	4.70E-01	0
500	0	3.90E-12	3.30E-01	0
750	0	2.95E-12	4.30E-01	2.78
1000	0	2.84E-12	4.40E+00	2.78

By investigating the results, the optimal values have been reached. The most efficient number of hidden layer is 500 and the most efficient number of iteration is 500 as shown in Table I and TableII. At the end of the process the error of training is calculated as 3.90E-12%, the error of test is 3.30E-01% and the error of diagnosis is 0%.

IV. CONCLUSION

In this study, the rotor fault effects on signals of power factor were analyzed by using FFT at steady state operation. For the analysis, experiments were performed for 3 different rotor faults and healthy motor conditions. The experimental results illustrate that the significant frequency components in frequency spectrum of power factor can be successfully applied for the broken bar diagnosis. The significant change depending on the rotor faults in frequency spectrum is used to be input matrix of supervised ANN. So, the classification was made. Consequently, the present study shows that the fault detection and classification from the power factor are quite feasible. The proposed method makes it possible to diagnose the faults, and discernment of them from each other with 100% accuracy.

ACKNOWLEDGMENT

The study has been supported by Scientific Research Project of Selcuk University.

ISBN: 978-988-19251-4-5
ISSN: 2078-0958 (Print); ISSN: 2078-0966 (Online)

REFERENCES

[1] A.H. Bonnett and G.C. Houkup, “Cause and analysis of stator and rotor faults in three-phase squirrel-cage induction motors”, IEEE Transactions on Industry Applications 28, No. 4, pp. 921–937, Aug. 1992.

[2] J. Penman and A. Stavrou, “Broken Rotor Bars Their Effect on the Transient Performance of Induction Machines”, IEE Proc.-Electr. Power Appl., Vol. 143, No. 6, pp. 449-457, Nov. 1996.

[3] H. Arabaci and O. Bilgin, “Automatic Detection and Classification of Rotor Cage Faults in Squirrel Cage Induction Motor”, Neural Computing And Applications, Vol. 19, No. 5, pp. 713-723, Jan. 2010.

[4] X. Ying, “Characteristic Performance Analysis of Squirrel Cage Induction Motor with Broken Bars”, IEEE Transactions on Magnetics, Vol. 45, No. 2, pp. 759-766, Feb. 2009.

[5] M. Haji and H.A. Toliyat, “Pattern recognition – a technique for induction machines rotor fault detection ‘Eccentricity and broken bar fault’ “, IEEE Industry Applications Conference, 2001. Industry Applications Conference, 2001. Thirty-Sixth IAS Annual Meeting. Vol. 3, pp. 1572-1578, 2001.

[6] B. Ayhan, M.-Y. Chow and M.-H. Song, "Multiple Discriminant Analysis and Neural-Network-Based Monolith and Partition Fault-Detection Schemes for Broken Rotor Bar in Induction Motors”, IEEE Transactions on Industrial Electronics, Vol. 53, No. 4, pp. 1298-1308, Aug. 2006.

[7] P.J.C. Branco, J.A. Dente and R.V. Mendes, “Using Immunology Principles for Fault Detection”, IEEE Transactions On Industrial Electronics, Vol. 50, No. 2, pp. 362-373, Apr. 2003.

[8] M. Benbouzid, M. Vieira and C. Theys, “Induction motors’ faults detection and localization using stator current advanced signal processing techniques,” IEEE Transactions on Power Electronics, vol. 14, no. 1, pp. 14–22, Jan. 1999.

[9] A. M. da Silva, R. J. Povinelli and N. A. O. Demerdash, " Induction Machine Broken Bar and Stator Short-Circuit Fault Diagnostics Based on Three-Phase Stator Current Envelopes”, IEEE Transactions On Industrial Electronics, Vol. 55, No. 3, pp. 1310-1318, Mar. 2008.

[10] C.H. De Angelo, G.R. Bossio and G.O. Garcia, " Discriminating broken rotor bar from oscillating load effects using the instantaneous active and reactive powers”, IET Electric Power Applications, Vol. 4, No. 4, pp. 281-290, Jan. 2010.

[11] M. Nemec, K. Drobnic, D. Nedeljkovic, R. Fišer and V. Ambrožic, “Detection of Broken Bars in Induction Motor Through the Analysis of Supply Voltage Modulation”, IEEE Transactions on Industrial Electronics, Vol. 57, No. 8, pp. 2879-2888, Aug. 2010.

[12] M. Eltabach, J. Antoni, G. Shanina, S. Zieba and X. Carniel, "Broken rotor bars detection by a new non-invasive diagnostic procedure", Mechanical Systems and Signal Processing, Vol. 23, pp. 1398-1412, 2009

ISBN: 978-988-19251-4-5
ISSN: 2078-0958 (Print); ISSN: 2078-0966 (Online)